IOP Conference Series: Materials Science and Engineering

PAPER • **OPEN ACCESS**

Development and trend of unified mechanism-based materials modelling for creep age forming of aluminium alloys

To cite this article: Xi Wang *et al* 2021 *IOP Conf. Ser.: Mater. Sci. Eng.* **1024** 012021

View the article online for updates and enhancements.

This content was downloaded from IP address 176.251.28.24 on 03/02/2021 at 10:55

Development and trend of unified mechanism-based materials modelling for creep age forming of aluminium alloys

Xi Wang[1,*], Yong Li[2], Baoguo Chen[3], Zhusheng Shi[1]

[1] Department of Mechanical Engineering, Imperial College London, London SW7 2AZ, UK

[2] School of Mechanical Engineering and Automation, Beihang University, Beijing 100191, China

[3] Shanghai Aircraft Manufacturing Co. Ltd, Shanghai 201324, China

* corresponding author: x.wang19@imperial.ac.uk

Abstract. Materials modelling plays an important role for sprinback compensation and tool surface design in creep age forming (CAF). This review aims to provide perspective on the development and trend of materials modelling for CAF of aluminium alloys. Recently proposed unified constitutive equations for creep-ageing behaviour of aluminium alloys during CAF by integrating microstructural evolution and hardening effects are reviewed. The modelling methods and developing trend to quantitively reflect the relationship between the microstructural evolutions and macro creep-ageing behaviour of materials during CAF are discussed.

1. Introduction

Creep age forming (CAF) was developed in the mid of 1980s and was initially used for fabricating of extra-large aircraft wing panel [1]. The upper-wing panel is normally formed with 7xxx aluminium alloys, due to the high strength and stiffness of the materials [2, 3]. For the lower wing panels, 2xxx aluminium alloys are chosen for their excellent fatigue and corrosion resistance performances, good balance of strength and toughness [3, 4].

It is of significance to establish proper constitutive models in predicting creep behaviour of materials in the forming and unloading stages during CAF process. By implementing the model in numerical simulation for springback compensation and surface die design, reduction of tooling cost and enhancement of forming efficiency can be achieved. In the early stage of studies, mathematically based material models were proposed to describe macro creep deformation, without linking microstructural evolution in CAF [4–6]. With further understanding of the effects of microstructural evolutions on macro creep deformation behaviour, unified mechanism based constitutive models were proposed, which revealed microstructure evolution features and their effects on creep deformation and age hardening in

Content from this work may be used under the terms of the Creative Commons Attribution 3.0 licence. Any further distribution of this work must maintain attribution to the author(s) and the title of the work, journal citation and DOI.
Published under licence by IOP Publishing Ltd

CAF. In this study, developments and trend of materials modelling for aluminium alloys in CAF are reviewed in a general perspective and its trend and challenge for future investigations are discussed.

2. Development of constitutive models for CAF

In 1991, Sallah et al. [5] proposed a constitutive equation by adopting Maxwell model to predict material's viscoelastic behaviour in CAF and was given in the form as:

$$\dot{\sigma} + F(\sigma, \varepsilon) = E\dot{\varepsilon},$$

where σ, ε, E stands for the stress, creep strain and Young's modulus of the material respectively. $F(\sigma, \varepsilon) = \sigma/\tau(\varepsilon)$ is the function to express stress relaxation in corresponding stress levels.

Later simplified power-law, exponential-law, sinh-law constitutive equations were widely adopted to describe creep behaviour in primary and secondary stages [4, 6–9]. The forms of these equations are listed in Table 1.

Table 1. Generation of constitutive equation forms

Power-law equation form	Exponential-law equation form	Sinh-law equation form
$\dot{\varepsilon} = A_1\sigma^n$	$\dot{\varepsilon} = A_2 \exp\left(\frac{\sigma^n}{B_1}\right)$	$\dot{\varepsilon} = A_3 \sinh\left(\frac{\sigma^n}{B_2}\right)$

In 2004, Ho et al. [10] proposed a mechanism based constitutive model which focused on predicting the creep deformation and age hardening behaviour of the material during CAF as shown in Table 2.

Table 2. Unified mechanism based constitutive model proposed by Ho et al. [10].

Microstructure variables	Strength evolution model	Creep strain-stress relationship
$\dot{r} = C_0\dot{\varepsilon}_c^{0.2}(Q-r)^{1/3}$	$\sigma_A = C_A r^{m_0}$ $\sigma_{SS} = C_{SS}(1+r)^{-m_1}$ $\sigma_y = \sigma_{SS} + \sigma_p$	$\dot{\varepsilon}_c = A\sinh\left\{B(\sigma-\sigma_A)(1-H)\left(\frac{C_{SS}}{\sigma_{SS}}\right)^n\right\}$ $\dot{H} = \frac{h}{\sigma^{0.1}}\left(1-\frac{H}{H^*}\right)\dot{\varepsilon}_c$

The model can well predict creep strain under different stress levels, as illustrated in Fig. 1(a). The model may be divided into three sub-models. In microstructure variables sub-model, the precipitate radius r is expressed in a rate form to reflect its growth during CAF. In strength evolution sub-model, yield strength (σ_y) is composed of precipitation hardening (σ_A) and solid solution hardening (σ_{ss}) of the material, as shown schematically in Fig. 1(b), which are related to the radius. A sinh law equation is adopted in the creep strain-stress relationship sub model. The variable H is introduced to represent the effect of dislocation hardening which is not directly considered in the microstructure sub-model.

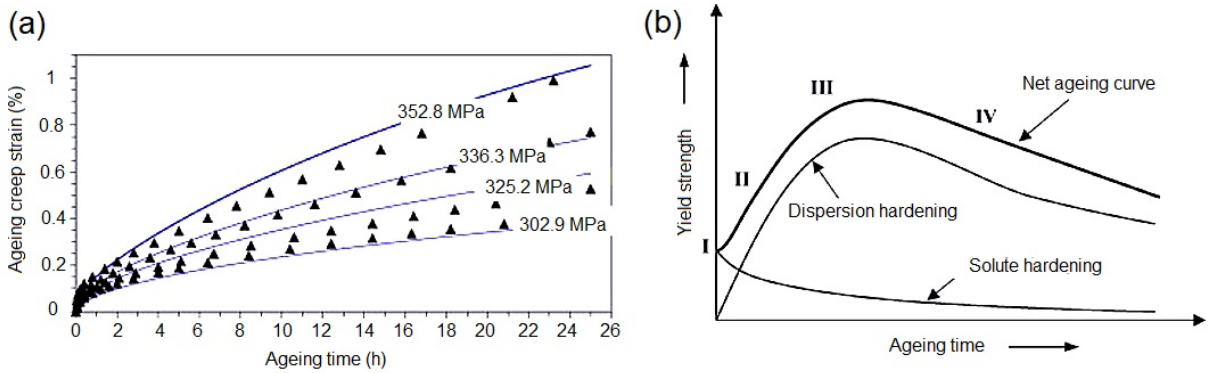


Fig. 1. Evolution of creep strain and strength during CAF: (a) Creep strains from modelling (lines) and experiment (symbols) ; (b) Schematic of yield strength evolution and contributors [10].

With further understanding of microstructural evolution during CAF, more microstructural variables are incorporated into material models. In 2010, Zhan et al. [11] proposed a constitutive model for CAF of AA7055 which can also be separated into three sub models as shown in Table 3. In this model, dislocation density ρ is modelled, considering its accumulation due to creep and reduction due to recovery. Its contribution to strength σ_{dis} is incorporated into the strength sub model, and its effect on creep strain is also considered. Fig. 2 shows a comparison of modelled results with experimental results for the evolution of creep strain and yield strength, showing good agreement.

Table 3. Unified mechanism based constitutive model proposed by Zhan et al [11].

Microstructure variables	Strength evolution model	Creep strain-stress relationship
$\dot{\bar{r}} = C_r(Q-\bar{r})^{m_3}(1+\gamma_0\bar{\rho}^{m_4})$ $\dot{\bar{\rho}} = A_3(1-\bar{\rho})\lvert\dot{\varepsilon}_{cr}\rvert - C_p\bar{\rho}^{m_5}$	$\dot{\sigma}_A = C_A\dot{\bar{r}}^{m_1}(1-\bar{r})$ $\dot{\sigma}_{ss} = C_{ss}\dot{\bar{r}}^{m_2}(\bar{r}-1)$ $\dot{\sigma}_{dis} = A_2\cdot n\cdot\bar{\rho}^{n-1}\dot{\bar{\rho}}$ $\sigma_y = \sigma_{ss} + \sqrt{\sigma_A^2+\sigma_{dis}^2}$	$\dot{\varepsilon}_{cr} = A_1\sinh\{B_1[\lvert\sigma\rvert(1-\bar{\rho}) - k_0\sigma_y]\text{sign}\{\sigma\}$

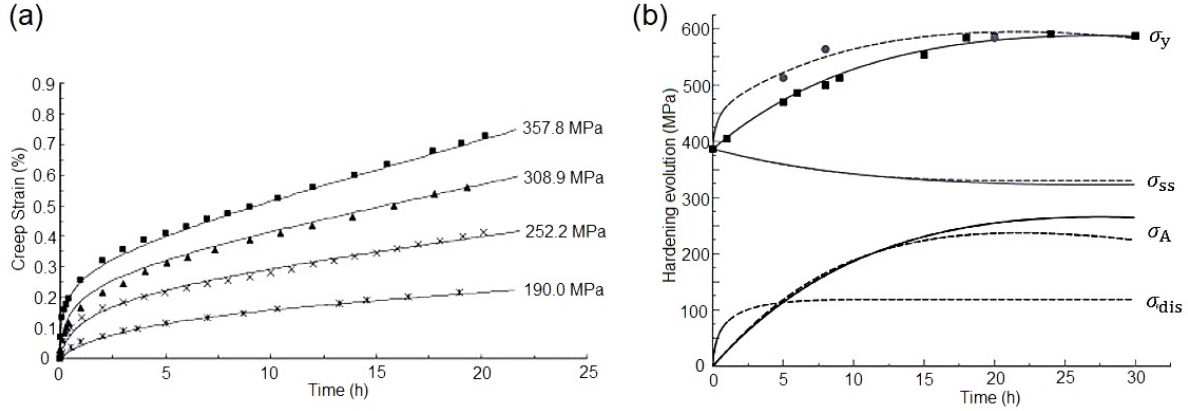


Fig. 2. Evolution of creep strain and strength during CAF of AA7055. (a) Creep strain curves from experiments (symbols) and modelling (lines). (b) Predicted evolution of yield strength and its components under 0 MPa (solid lines) and 250 MPa (dash lines), and corresponding experimental data (symbols) [11].

Considering the precipitate morphology, Zhang et al. [12] proposed a new constitutive model for creep-ageing of aluminium alloys containing rod or plate shape precipitates in 2013, as listed in Table 4. The volume fraction f_v, morphology parameter l (diameter for plate and length for rod) and aspect ratio q of the precipitates were employed to describe the evolution of plate- and rod-shaped precipitates during CAF. The effect of ageing temperature on creep deformation are expressed with the term $exp(-Q/RT)$ in the creep strain-stress relationship.

Table 4. Unified mechanism based constitutive model proposed by Zhang et al [12].

Microstructure variables	Strength evolution model	Creep strain-stress relationship
$\dot{\bar{f}}_v = \frac{C_1 l^{n_1} l}{q^{n_2}}(1-\bar{f}_v)^{m_1}$ $\dot{l} = C_2(Q_1-l)^{m_2}(1+k_1\bar{\rho}_m^{n_3}\dot{\bar{\rho}}_m)\exp\left(\frac{-Q_2}{RT}\right)$ $\dot{\bar{\rho}}_m = C_3(Q_3-\bar{\rho}_m)\dot{\varepsilon}_c$ $q = \frac{C_4}{\exp[k_2(T-T^*)^2 + k_3(t-t^*)^2]}$	$\sigma_p = C_{\text{ppt}}(q\bar{f}_v)^{n_4} l^{n_5}$ $\sigma_{\text{ss}} = C_{\text{ss}}(1-\bar{f}_v)^{m_3}$ $\sigma_{\text{dis}} = C_{\text{dis}}\bar{\rho}_m^{1/2}$ $\sigma_{\text{y}} = \sigma_0 + \sigma_{\text{ss}} + \sigma_{\text{p}} + \sigma_{\text{dis}}$	$\dot{\varepsilon}_c = A\sinh\left(\frac{B\sigma}{\sigma_y}\right)^n \exp\left(-\frac{Q}{RT}\right)$

More recently, Li et al. [13] investigated the creep-ageing behaviour of Al-Cu-Li alloy AA2050 and revealed the characteristics of asymmetric creep behaviour under tension and compression, double

primary creep feature, and initial reversion in age hardening. They proposed an advanced constitutive model to describe the creep-ageing behaviour with above characteristics, as shown in Table 5 [13]. This model has disassociated creep strain rate at ageing temperature with room temperature yield strength, both of which are related to microstructural variables.

Table 5. Unified mechanism based constitutive model proposed by Li et al [13].

Microstructure variables	Strength evolution model	Creep strain-stress relationship
$\dot{\bar{\rho}} = A_1(1-\bar{\rho})\lvert\dot{\varepsilon}_{cr}\rvert^{m_1} - C_p\bar{\rho}^{m_2}$ $\dot{\bar{r}}_n = C_r(Q-\bar{r}_n)^{m_3}(1+\gamma_0\bar{\rho}^{m_4})$ $\dot{\bar{r}}_d = -\frac{C_{r1}}{\bar{r}_d}$ $\dot{\bar{c}} = -A_2(\bar{c}-\bar{c}_a)(1+\gamma_0\bar{\rho}^{m_4})$	$\dot{\sigma}_{p-n} = C_a\dot{\bar{r}}_n^{m5}\left(1-\bar{r}_n^{m_6}\right)$ $\dot{\sigma}_{p-d} = C_{a1}\bar{r}_d^{m}\dot{\bar{r}}_d$ $\dot{\sigma}_{ss} = -C_{SS}\lvert\dot{\bar{c}}\rvert^{m_8}(\bar{c}-\bar{c}_a)$ $\dot{\sigma}_{dis} = A_3 n\bar{\rho}^{n-1}\dot{\bar{\rho}}$ $\sigma_y = \sigma_{ss} + \sqrt{\sigma_{dis}^2 + \left(\sigma_{p-d}^2 + \sigma_{p-n}^2\right)}$	$\dot{\varepsilon}_{cr} = A_4\sinh\left\{B_1\left[\left(\lvert\sigma\rvert - \sigma_{th_0}\right)(1-H)\right]\right\}\text{sign}\,(\sigma)$ $H = k_1\bar{\rho} + k_2\bar{c} + k_3\left(\bar{r}_n + \beta^{1/2}\bar{r}_d\right)$

In microstructure variables sub model, two types of precipitates were considered, new precipitates (r_n) and pre-existing (or dissolving) precipitates (r_d). The latter dissolves at the initial stage, leading to the reversion in age hardening Other microstructural variables include dislocation density (ρ) and solute concentration (c) in the normalised forms which evolves with ageing progress.

This model is characterised for adequate prediction of asymmetric creep behaviour under tension and compression and double primary creep feature exhibited in AA2050. A sinh law equation is used for the strain rate-stress relationship. By introducing the variable *H* in the equation, the asymmetric creep behaviour is well captured after calibrating constants *k1*, *k2*, and *k3* with experimental data, as shown in Fig. 3. The modelled results agree well with the experimental data and have the double primary creep feature. This model is versatile and has been shown to be adoptable to natural ageing and artificial ageing as well as CAF of other aluminium alloys [14].

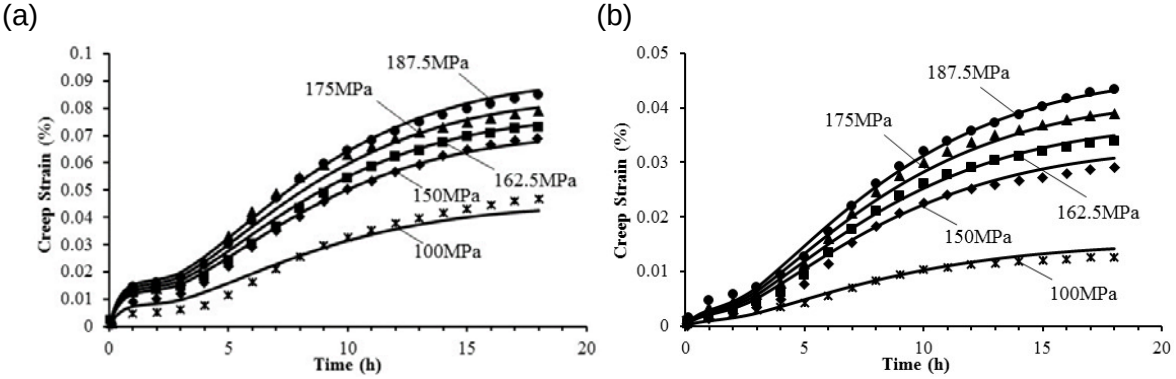


Fig. 3. Comparison of experimental (symbols) and modelled (lines) creep strain curves for AA2050 under (a) tension and (b) compression during creep-ageing [13].

Material model has also been be developed for creep-ageing with stress large than the initial yield the stress. In 2018, Ma et al. [15] proposed a unified model to describe the creep deformation in stress levels under and beyond its initial yield stress. In this model, a bi-precipitates model was created to represent the evolution of plate shaped θ'' and θ' precipitates having different diameter and thickness. Correspondingly, the strength contribution of precipitation hardening σ_p was divided into contribution of shearable precipitates $\sigma_{shearable}$ and non-shearable precipitates $\sigma_{non-shearable}$. The creep strain-stress relationship is given as

$$\dot{\boldsymbol{\varepsilon}}_{\boldsymbol{c}} = \boldsymbol{c}_{\boldsymbol{11}}\left(\frac{\boldsymbol{\sigma}+\boldsymbol{c}_{\boldsymbol{12}}(\boldsymbol{\sigma}-\boldsymbol{\sigma}_{\boldsymbol{IY}})}{(\boldsymbol{\sigma}_{\boldsymbol{\rho}}+\boldsymbol{k}_{\boldsymbol{1}}\boldsymbol{\sigma}_{\boldsymbol{shearable}}+\boldsymbol{k}_{\boldsymbol{2}}\boldsymbol{\sigma}_{\boldsymbol{non-shearable}})^{\boldsymbol{n}_{\boldsymbol{4}}}}\right) \quad (1)$$

where σ_{IY} is the yield strength in initial state. This equation can describe the creep strain evolution under the stress beyond the yield strength of the material.

3. Derivation of unified mechanism based constitutive models

CAF is a heat treatment and time dependent forming method in which the states of microstructure features are varying with different treatment parameters. These microstructure features, including size and volume fraction of precipitation and dislocation density, are found to affect the material strength evolution and creep deformation.

3.1 Microstructure variables

Studies have shown that dislocations influence growth and density increase of precipitates [16–18]. For heterogenous nucleation, dislocations provide crystallographic defects which lower the total free energy required for the nucleation of precipitates.

Kocks-Mecking-Estrin (KME) [19, 20] equation is widely adopted in characterising the relationship between evolution of statistically stored dislocation density ρ_s (i.e. excluding geometric necessary dislocation density induced by Orowan loops) and plastic strain ε_p . This equation is given as

$$\frac{\partial \rho_s}{\partial \dot{\varepsilon}_p} = \boldsymbol{M}(\boldsymbol{k_1}\sqrt{\boldsymbol{\rho_s}} - \boldsymbol{k_2}\boldsymbol{\rho_s}) \quad (2)$$

where M is the Taylor factor, k_1 is the constant related to the rate of dislocation storage, and k_2 is the constant associated with dynamic recovery.

Several other equations were proposed based on the modification of KME model such as [21]

$$\dot{\boldsymbol{\rho}} = \boldsymbol{K_1}\sqrt{\boldsymbol{\rho}}\dot{\boldsymbol{\varepsilon}}_{\boldsymbol{cr}} - \boldsymbol{K_2}\boldsymbol{\rho}(\dot{\boldsymbol{\varepsilon}}_{\boldsymbol{cr}})^{\boldsymbol{N}} \quad (3)$$

and [11, 13]

$$\dot{\bar{\boldsymbol{\rho}}} = \boldsymbol{A_1}(\boldsymbol{1}-\bar{\boldsymbol{\rho}})|\dot{\boldsymbol{\varepsilon}}_{\boldsymbol{cr}}|^{\boldsymbol{m_1}} - \boldsymbol{C_p}\bar{\boldsymbol{\rho}}^{\boldsymbol{m_2}} \quad (4)$$

where $\bar{\rho}$ is the normalised dislocation density, $\dot{\varepsilon}_{cr}$ is the strain rate in creep aging, and the additional term $-C_P\bar{\rho}^{m_2}$ stands for the effect of dislocation recovery.

A cubic coarsening law to approximate the evolution kinetics was proposed by Ashby [22] based on the assumption that the precipitate growth in respect of ageing time is a single peak curve:

$$\boldsymbol{r(t)^3} - \boldsymbol{r_0}^3 = \frac{\boldsymbol{c_1 t}}{\boldsymbol{T}}\boldsymbol{\exp}\left(-\frac{\boldsymbol{Q_A}}{\boldsymbol{RT}}\right) \quad (5)$$

where $r(t)$ is the average precipitates radius at ageing time t, r_0 refers to the radius at the beginning time t=0. Q_A is the activation energy and c_1 is material constant depending on the matrix composition.

Based on the above equation, a normalised precipitate radius $\bar{r}_n = r_n/r_c$ was introduced [11, 13]. r_n is the average precipitate radius at current ageing time, r_c is the critical radius at peak-ageing state. With corresponding mathematical transformation, the general modified equation can be derived as

$$\dot{\bar{\boldsymbol{r}}}_{\boldsymbol{n}} = \boldsymbol{C_r}(\boldsymbol{Q}-\bar{\boldsymbol{r}}_{\boldsymbol{n}})^{\boldsymbol{m_3}}(\boldsymbol{1}+\boldsymbol{\gamma_0}\bar{\boldsymbol{\rho}}^{\boldsymbol{m_4}}) \quad (6)$$

where Q is the factor representing the saturation state of precipitate growth; Cr, γ_0, m_3 and m_4 are material constants. The term $(1+\gamma_0\bar{\rho}^{m_4})$ represents the effect of dislocation density.

Two parameters are required to quantify the morphology of the precipitates. For rod/needle shaped precipitate, an aspect ratio q is defined with length l and section diameter d as $q = l/d$ [12]. Similarly, Ma et al. [15] adopted d and t as two morphology parameters to describe the diameter and thickness of plate shape precipitates respectively.

Precipitate volume fraction has effects on precipitation hardening and solid solution hardening in

ageing. Some models treat this effect as a function of precipitate radius and therefore do not express it explicitly [13]. Others introduce explicit equations for precipitate volume fraction [12, 15].

As a basic form to express volume fraction evolution, Kolmogorov-Johnson-Mehl-Avrami (JMAK) equation has been adopted as a continuous process to fit the evolution of precipitate volume fraction with experimental data [23]. The form of the JMAK equation is given as

$$\boldsymbol{f_v = 1 - exp\,(-Kt^n)} \quad (7)$$

where f_v is the relative transformed precipitate volume fraction, t is the ageing time, K and n are constants.

3.2 Strength evolution model

Shercliff and Ashby [24] proposed a precipitation hardening model, considering the interactions between dislocations and precipitates:

$$\boldsymbol{\sigma_A = c_3 f^m r^n;\ \sigma_B = c_4 \frac{f^{1/2}}{r}} \quad (8)$$

where σ_A stands for the strengthening effect caused by dislocation interaction with weak precipitate and σ_B is for the strong precipitate. The equations show that the strengthening effect will increase with volume fraction, while the effect of precipitate radius depends on shearing and bypassing interaction mechanisms. A harmonic equation in the form of $\sigma_p = ({\sigma_A}^{-1} + {\sigma_B}^{-1})^{-1}$ can be adopted to combine the two interaction effects, as shown by [13].

In solid solution hardening, the strength of the material is enhanced with the obstructing of dislocation motion by solute atoms [25]. The yield strength contribution from dislocation glide resistance caused by solutes at normalised concentration $\bar{c}$ can be expressed as [24]:

$$\boldsymbol{\sigma_{ss} = \alpha \bar{c}^{2/3}} \quad (9)$$

where α is a material constant related to precipitate size and modulus of the solute.

By substituting $\bar{c}$ with the relationship with relative volume fraction f_v proposed by Shercliff and Ashby [24] , a general form can be derived as:

$$\boldsymbol{\sigma_{ss} = C_{ss}(1 - f_v)^{2/3}} \quad (10)$$

where C_{ss} is material constant. This form of equation was widely adopted in investigations of strength contribution of solid solution hardening [18, 21, 26, 27] and was proved to be an adequate approximation.

The dislocation hardening is generally modelled as a function of the dislocation density [15, 28]:

$$\boldsymbol{\sigma_{dis} = M\alpha\mu b\rho^{1/2}} \quad (11)$$

A simplified general version is given as in Eq. (12), where n is a constant:

$$\boldsymbol{\sigma_{dis} = A_3 \bar{\rho}^n} \quad (12)$$

All the above strength components, i.e., $\sigma_p, \sigma_{ss}, \sigma_{dis}$, contribute to the yield strength of the material. Their contributions, however, may be represented in different ways. Some researchers use linear summation model for the overall macroscopic yield strength σ_y as follows [26, 29–31]:

$$\boldsymbol{\sigma_y = \sigma_i + \sigma_{ss} + \sigma_p + \sigma_{dis}} \quad (13)$$

However, the linear summation equation can lead to double counting of precipitation hardening and dislocation hardening [31, 32]. Hence, the addition law strength model is used by some other researchers with variable n varying between 1 and 2 [11, 13, 21]:

$$\boldsymbol{\sigma_y = \sigma_i + \sigma_{ss} + (\sigma_p{}^n + \sigma_{dis}{}^n)^{1/n}} \quad (14)$$

4. Discussion

By referencing a basic constitutive model structure, more comprehensive models in aspects of micro

and macro have been proposed. Initially, precipitation hardening and solid solution hardening were considered in the model proposed by Ho et al. [10]. Later, Zhan et al. [11] incorporated the effect of dislocation density on evolution of strength and creep strain during CAF.

In more recent modelling of CAF, more features in microstructural evolution have been considered, e.g. the dissolution of pre-existing precipitates or clusters, and both shearing and bypassing interaction mechanisms between precipitates and dislocations [13]. The former leads to the prediction of the strength reversion at the initial stage. Also, new variables were introduced in the model to reflect the material's macro asymmetric creep deformation under tension and compression [13]. These advanced models had proved their usability and significance in predicting the material behaviour in CAF and springback compensation in forming process. It was also shown that such material model may be used for CAF of other alloys or other heat treatments by adopting related mechanisms [14].

In recent years, advanced aluminium alloys which exhibit superior performances in material strength, weight reduction, and corrosion resistance are continually invented and introduced into the market. The 3rd generation Al-Li series alloys such as AA2050, AA2060, AA2090 can be viewed as good examples of newly invented alloys.

New requirements have been raised for the constitutive equations to reflect characteristics which have not been considered in predecessors and recently invented alloys. For Al-Cu and Al-Li alloys, anisotropy is an unfavoured issue existed in each generation of the alloys [33–35]. The dependency of anisotropy in creep-ageing of textured Al-Cu-Mg alloy was studied [35], which finds obvious anisotropic behaviour in creep strain. Anisotropic creep deformation of AA2050 in longitudinal and transvers directions was observed, and modelled using the same constitutive equation but with different values for some material constants [36]. The effect of anisotropic creep strains on the springback during CAF was also numerically investigated in the study. It is of significance to study the effect of anisotropy in CAF fabrication and a unified model to illustrate its effect is needed. In addition, double ageing treatment is also being proposed to be applied in Al-Li alloys to enhance the formability and meet the component contour requirements [33]. Constitutive models adequate to describe this double ageing treatment for Al-Li alloys also needs to be further studied.

5. Conclusions

1. Based on a basic constitutive model structure, more comprehensive material responses in aspects of microstructural evolution and macro behaviour in CAF have been taken into consideration. Some equations describing evolution of microstructural variables and material strength are originated from earlier studies of ageing behaviour of materials.
2. With advanced alloys being introduced into the market and rapid developments of FEM in recent years, proposing constitutive models which can reflect anisotropic characteristics and responses in innovative CAF process becomes future needs and development trends.
3. More internal variables are employed in new material models in order to capture the mechanisms and predict material behaviours in CAF more accurately. It is of significance to develop and adopt proper algorithms to meet the requirements of calibrating material constants for more complexed models.

Acknowledgement

Financial support from Commercial Aircraft Corporation of China (COMAC) is gratefully

acknowledged.

References

[1] Holman MC. J. Mech. Work. Technol. 1989;20:477–88.
[2] Denzer, D. K., Rioja, R. J., Bray, G. H., et al. The Evolution of Plate and Extruded Products with High Strength and Fracture Toughness. Cham: Springer International Publishing; 2016. p. 587–592.
[3] Prasad NE, Gokhale AA, Wanhill RJH. Aluminum-lithium alloys: Processing, properties, and applications. Oxford: Elsevier Butterworth-Heinemann; 2014.
[4] Guines D, Gavrus A, Ragneau E. Int J Mater Form. 2008;1:1071–4.
[5] Sallah M, Peddieson J, Foroudastan S. J. Mater. 1991;28:211–9.
[6] Idem K, Peddieson J. J. Manuf. Sci. Eng. 2005;127:165–72.
[7] Seidman D, Marquis E, Dunand D. Acta Mater. 2002;50:4021–35.
[8] Zerilli FJ, Armstrong RW. J. Appl. Phys. 1987;61:1816–25.
[9] Huang C, Wei M, Lee S. J. Appl. Phys. 2011;27:1093–102.
[10] K.C. Ho, J. Lin, T.A. Dean. J. Mater. Process. 2004;153-154:122–7.
[11] Zhan L, Lin J, Dean TA, Huang M. Int. J. Mech. Sci. 2011;53:595–605.
[12] Zhang J, Deng Y, Zhang X. Mater. Sci. Eng. A. 2013;563:8–15.
[13] Li Y, Shi Z, Lin J, Yang YL, Rong Q, Huang BM, et al. Int. J. Plast. 2017;89:130–49.
[14] Li Y, Shi Z, Lin J, Yang YL, Rong Q, Mater. Des. 2017;122:422-432.
[15] Ma Z, Zhan L, Liu C, Xu L, Xu Y, Ma P, et al. Int. J. Plast. 2018;110:183–201.
[16] Lin Y, Lu C, Wei CY, Zheng ZQ. Mater. Charact. 2018;141:163–8.
[17] Zhao TZ, Jin L, Xu Y, Zhang SH. Mater. Sci. Eng. A. 2020;771.
[18] Zhang J, Wang C, Zhang Y, Deng YL. J. Alloys Compd. 2018;764:452–9.
[19] Kocks UF. J. Eng. Mater. Technol. 1976;98:76–85.
[20] Estrin Y. J. Mater. Process. 1998;80-81:33–9.
[21] Fribourg G, Brechet Y, Deschamps A, Simar A. Acta Mater. 2011;59:3621–35.
[22] Ashby MF. Phil. Mag. 1970;21:399–424.
[23] Nie JF, Muddle BC. J Phase Equilibria Diffus. 1998;19:543–51.
[24] Shercliff HR, Ashby MF. Acta Metall. Mater. 1990;38:1789–802.
[25] Labusch R. Phys. Stat. Sol(b). 1970;41:659–69.
[26] Yang Y, Zhan L, Shen R, Yin X, Li X, Li W, et al. Mater. Sci. Eng. A. 2017;683:227–35.
[27] Esmaeili S, Lloyd DJ, Poole WJ. Acta Mater. 2003;51:2243–57.
[28] Rodgers BI, Prangnell PB. Acta Mater. 2016;108:55–67.
[29] Myhr OR, Grong O, Pedersen KO. Metall Mater Trans A. 2010;41:2276–89.
[30] Yang YL, Zhan LH, Xu XL. Strength Mater. 2016;48:23–31.
[31] Cheng LM, Poole WJ, Embury JD, Lloyd DJ. Metall Mater Trans A.2003; 34:2473–81.
[32] Poole WJ, Wang X, Lloyd DJ, Embury JD. Philos Mag. 2005;85:3113–35.
[33] Bodily B, Heinimann M, Bray G, et al. SAE Tech. 2012.
[34] Abd El Aty A, Xu Y, Guo X, et al. J. Adv. Res. 2018;10:49–67.
[35] Chen X, Zhan L, Xu Y, et al. Mater. Charact. 2020;168:110539.
[36] Tong CP, Li Y, Shi Z. Procedia Manuf. 2020;50:241–247.